sustainability

MDPI

Article

Estimation and Differential Analysis of the Carbon Sink Service Radius of Urban Green Spaces in the Beijing Plain Area

Shurui Gao, Peiyuan Tao, Zhiming Zhao, Xinyue Dong, Jiayan Li and Peng Yao *

School of Landscape Architecture, Beijing Forestry University, Beijing 100083, China
* Correspondence: chinayp@bjfu.edu.cn

Abstract: Enhancing the carbon sink capacity of urban green spaces is considered an effective means of reducing carbon dioxide concentration. This study, employing xCO_2 as a key indicator and utilizing buffer analysis, estimated the carbon sink service radius of urban green spaces. Using spatial zoning and multifactor analysis, this research statistically analyzed 15 indicators, exploring the differences in carbon sink service radius from both the dimensions of urban green spaces and urban zones. The findings indicate that the carbon sink service radius is a result of the combined effect of urban green spaces and adjacent urban areas. Urban green space area, the NPP (net primary productivity) of urban zones, forest proportion, and grassland proportion are positively correlated with the carbon sink service radius, and the correlation degree is 0.12, 0.095, 0.121, and 0.125, respectively. The proportion of grassland and the proportion of impervious area in the city have a significant negative correlation with the carbon sink service radius, and the correlation degree is −0.074 and −0.081, respectively. This research holds significant implications for enhancing the carbon sink capacity of urban green spaces, adjusting land use patterns, and promoting the sustainable development of cities.

Keywords: urban green space; carbon sink; spatial service radius; sustainable urban planning; Beijing plain area

Citation: Gao, S.; Tao, P.; Zhao, Z.; Dong, X.; Li, J.; Yao, P. Estimation and Differential Analysis of the Carbon Sink Service Radius of Urban Green Spaces in the Beijing Plain Area. *Sustainability* **2024**, *16*, 1406. https://doi.org/10.3390/su16041406

Academic Editor: Silvia Fiore

Received: 12 December 2023
Revised: 29 January 2024
Accepted: 6 February 2024
Published: 7 February 2024

1. Introduction

The rapid development of cities and extensive energy consumption have led to a continuous increase in carbon dioxide (CO_2) emissions, causing global concerns about issues such as air pollution and global warming [1]. Efforts to reduce the concentration of CO_2 in the atmosphere mainly focus on decreasing CO_2 emissions. This involves various strategies, including enhancing energy efficiency and transitioning to low-carbon or zero-carbon fuels [2–4]. Additionally, people utilize negative emission technologies (NETs) to extract carbon from the atmosphere and safely store it, contributing to carbon emission reduction [5,6]. These technologies encompass carbon capture and storage (BECCS), afforestation, reforestation, soil carbon sequestration, and direct air carbon capture and storage (DACCS) [7–9]. Against this backdrop, leveraging the carbon sink capacity of ecological spaces by harnessing plants' ability to absorb atmospheric CO_2 through photosynthesis becomes a crucial means of achieving carbon peaking and carbon neutrality goals [10].

National and local policies emphasize the construction of urban green spaces and the enhancement of their carbon sink capacity. In September 2021, the Chinese government outlined requirements to strengthen ecosystem carbon sink capacity and increase ecosystem carbon sink increments [11]. In October 2022, the Beijing municipal government proposed a coordinated approach to promote spatial reduction and ecological space increment, advancing carbon sequestration in forests and green spaces [12]. Urban and rural green spaces, as essential spatial carriers for carbon sequestration, play a crucial role in carbon fixation, oxygen release, temperature reduction, humidity increase, and the alleviation of the urban heat island effect [13]. This holds practical significance for achieving dual carbon goals. The Beijing plain area, as a major urban construction zone and a primary space for carbon emissions, has an urgent need for increased carbon sequestration and emission reduction. Therefore, conducting relevant research on the carbon sink efficiency of green spaces in the Beijing plain area can provide more in-depth and comprehensive support for urban carbon reduction and ecosystem services.

Recently, many scholars have simulated and calculated the net primary productivity (NPP) of vegetation in Beijing, exploring the spatiotemporal patterns of Beijing's NPP [14] and its response to climate change [15]. They have also simulated the impact of land use changes on NPP under various scenarios [16], providing preliminary insights into Beijing's carbon sink capacity and influencing factors. Research indicates that the diversity and comprehensive layout of urban land use alter the spatial relationship between carbon emissions and sequestration concerning the location, form, and layout changes of green spaces [17]. Therefore, conducting calculations of the carbon sink efficiency and studying the impact range of green spaces in the highly urbanized Beijing plain area will help better understand the significance of urban green space construction in terms of "increasing carbon sink" and the effectiveness of "carbon reduction".

Researchers have separately calculated carbon emissions and sequestration at the administrative district [18], urban [19], and city-cluster scales [20], quantitatively assessing the supply–demand relationship of carbon sequestration services. However, these studies have generally overlooked the atmospheric flow and transformation of CO_2, and have not fully reflected the actual urban CO_2 concentration. Resorting to xCO_2 data measured by the OCO-2 satellite is a commonly used method for spatially studying CO_2 concentration [21]. For example, scholars have utilized xCO_2 data to analyze the spatial distribution characteristics of CO_2 concentration along urban–rural gradients in Chinese cities [22], and explore the spatiotemporal variations, influencing factors, and driving effects of CO_2 concentration in the study region [23]. Therefore, this study, using xCO_2 as a key dataset, analyzes the spatial variation of CO_2 concentration and explores the actual effects of urban green spaces on reducing the concentration of CO_2 in surrounding urban areas. This will contribute to providing more specific scientific foundations for urban planning and green space design.

Current research indicates that terrestrial carbon sinks are collectively determined by various processes in the carbon cycle of terrestrial ecosystems at different temporal and spatial scales [24]. Due to regional conditions and different carbon sink source types, there is considerable variation in carbon balances [25], making carbon sink services regionally specific. Simultaneously, the supply levels of ecological and social services provided by urban green spaces not only depend on the total green space quantity but are also closely related to their spatial configuration [26]. The urban green space service radius is commonly used as a measure of the rationality of green space spatial configuration in cities. Moreover, an increasing number of scholars employ the buffer analysis method to investigate green space accessibility [27], cooling effects [28], and associations with health and behavioral outcomes [29]. Therefore, based on the fluidity of carbon, the regionality of carbon sink services, and the service radius of urban green spaces, this study introduces the concept of the "carbon sink service radius": urban green spaces, through carbon sink processes, induce changes in atmospheric CO_2 concentration. Taking urban green spaces as the center, the maximum range within which the CO_2 concentration in the surrounding urban areas can be reduced is defined as the carbon sink service radius of urban green spaces. This concept emphasizes and quantifies the crucial role of urban green spaces in improving atmospheric CO_2 concentration. The carbon sink service radius allows us to focus on regional differences in carbon sink services and gain a more comprehensive understanding of carbon sink characteristics in different urban areas.

Revealing the fundamental reasons for the differences in the carbon sink service radius of urban green spaces can provide a deeper understanding of their role in reducing atmospheric CO_2 concentration, thereby better harnessing the role of urban green spaces in mitigating climate change and improving the ecological environment. Pearson correlation analysis is a commonly used method for exploring driving factors. Previous scholars have applied Pearson correlation analysis to the study of driving factors for carbon sinks and emissions. Research indicates that, due to the combined influence of carbon sinks and emissions on urban CO_2 concentration, factors such as green space area, net primary productivity (NPP), the normalized difference vegetation index (NDVI), and vegetation cover type contribute to variations in the carbon sink capacity of urban green spaces [30–32]. Additionally, land use types and nighttime light indices are often studied as influencing factors for carbon emissions [33,34].

This study combines these research methods, using CO_2 concentration as an indicator and urban green spaces as the center. It employs the buffer analysis method to calculate the carbon sink service radius of urban green spaces. Furthermore, factors related to carbon sinks and emissions are selected, and Pearson correlation analysis is applied to analyze their correlation with the carbon sink service radius. The specific objectives are (1) to calculate the carbon sink service radius and quantify the actual effect of urban green spaces on reducing CO_2 concentration in surrounding urban areas; (2) to determine the causes of differences in the carbon sink service radius and reveal the carbon sink service mechanism of urban green spaces; and (3) to provide recommendations for the planning, layout, and construction of urban green spaces in the Beijing plain area.

2. Materials and Methods

2.1. Overview of the Study Area

The Beijing plain area covers an approximate area of 6338 km^2, constituting 38.62% of the total administrative area of Beijing [35]. According to the "Protection Plan for the Shallow Mountainous Areas of Beijing" and related studies, the Beijing plain area encompasses plains and plateaus with elevations ranging from 0 to 100 m within the municipal boundaries [36]. Thus, the 100 m contour line is utilized as the boundary to delineate the research scope of the Beijing plain area (Figure 1).

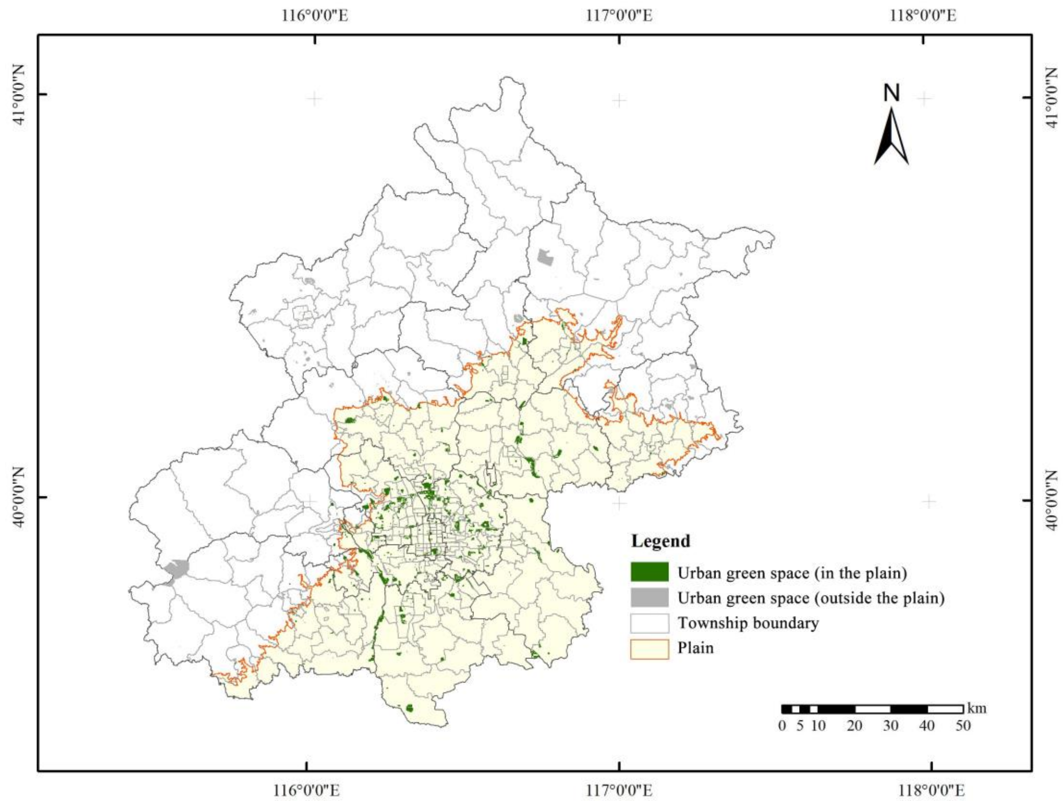

Figure 1. Study area and urban green space of the Beijing plain.

Blessed with a favorable geographic location and abundant resources, the Beijing plain area serves as the primary carrier for the core and urban functions of the capital, boasting a relatively high level of urbanization. This region is adorned with numerous green spaces such as parks, forests, and wetlands, making it a vital system within the urban scope with direct carbon sequestration and indirect emission reduction functions. It serves as a crucial foundation for enhancing the carbon sink capacity of urban ecosystems [37]. The Beijing plain area stands out as a representative region for studying urban carbon sinks.

2.2. Data Acquisition and Preprocessing

2.2.1. Urban Green Space Data

Using the ArcGIS 10.5 platform, the 100 m contour line was extracted from the Beijing 30 m DEM elevation data to define the boundary of the Beijing plain area. The 2020 Beijing urban green space vector data were downloaded from WeServer (www.rivermap.cn, accessed on 2 March 2023), selecting 532 green spaces within the plain area, including various urban parks, specialized parks, suburban parks, forest parks, and scenic areas.

2.2.2. Net Primary Productivity (NPP)

The study utilized the Beijing 30 m net primary productivity (NPP) data from the GISRS platform (www.gisrs.cn, accessed on 2 March 2023). Widely applied in ecosystem carbon sink studies, these data are based on the CASA model [38]. It estimates vegetation's net growth status by considering solar radiation absorption and utilization by vegetation. The estimated NPP is expressed using two factors: absorbed photosynthetically active radiation (APAR) and actual light use efficiency (ε). The formula is as follows:

$$NPP(x, t) = APAR(x, t) \times \varepsilon(x, t)$$

where x represents an individual pixel, t denotes the month, APAR(x, t) signifies the absorbed photosynthetically active radiation in grams of carbon per square meter, and ε(x, t) indicates the actual light use efficiency in grams of carbon per megajoule.

2.2.3. Carbon Dioxide Concentration Data (xCO_2)

The carbon dioxide concentration data used in the study were obtained from the OCO-2_L2_Lite_SIF 10 r dataset provided by the EARTHDATA platform. After filtering the raw data based on the study area and data quality, the global carbon dioxide concentration data from 1 January 2020 to 31 December 2020 were selected. Subsequently, Python 3.7.8 software was employed to read the daily data, which were then imported into ArcGIS 10.5 for further processing. Monthly and annual CO_2 data were calculated, and the data were clipped to the boundary of Beijing city. The final step involved visualization and obtained raster data with a spatial resolution of 880 × 880 m.

2.2.4. Vegetation Cover Type

For the feasibility of data acquisition and the effectiveness of the study, 2019 satellite imagery of Beijing with a resolution of 30 m was selected. Preprocessing in the ENVI platform included cropping, mosaicking, atmospheric correction, and radiometric calibration. Unsupervised classification was performed to categorize the imagery into six vegetation cover types: impervious surface, water bodies, grassland, woodland, cultivated land, and unused land. The resulting vegetation cover type map had a resolution of 30 m. Through data comparison and validation, the Kappa coefficient was 0.91, meeting accuracy requirements.

2.2.5. Other Data

In the study of carbon sink service radius differences, factors related to carbon emission and sequestration, such as the normalized difference vegetation index (NDVI) and nighttime light data, were considered in addition to NPP and vegetation cover type. NDVI serves as an optimal indicator of vegetation growth and coverage, exhibiting sensitivity to NPP dynamics and closely correlating with carbon sink capacity [39]. Nighttime light data reflect human activity intensity and are commonly used in carbon emission estimation [40].

In ArcGIS 10.5, all raster data considered as influencing factors were reconstructed to a 30 m resolution. Figure 2 shows the spatial distribution and distribution of each impact factor. Table 1 summarizes the sources of all data.

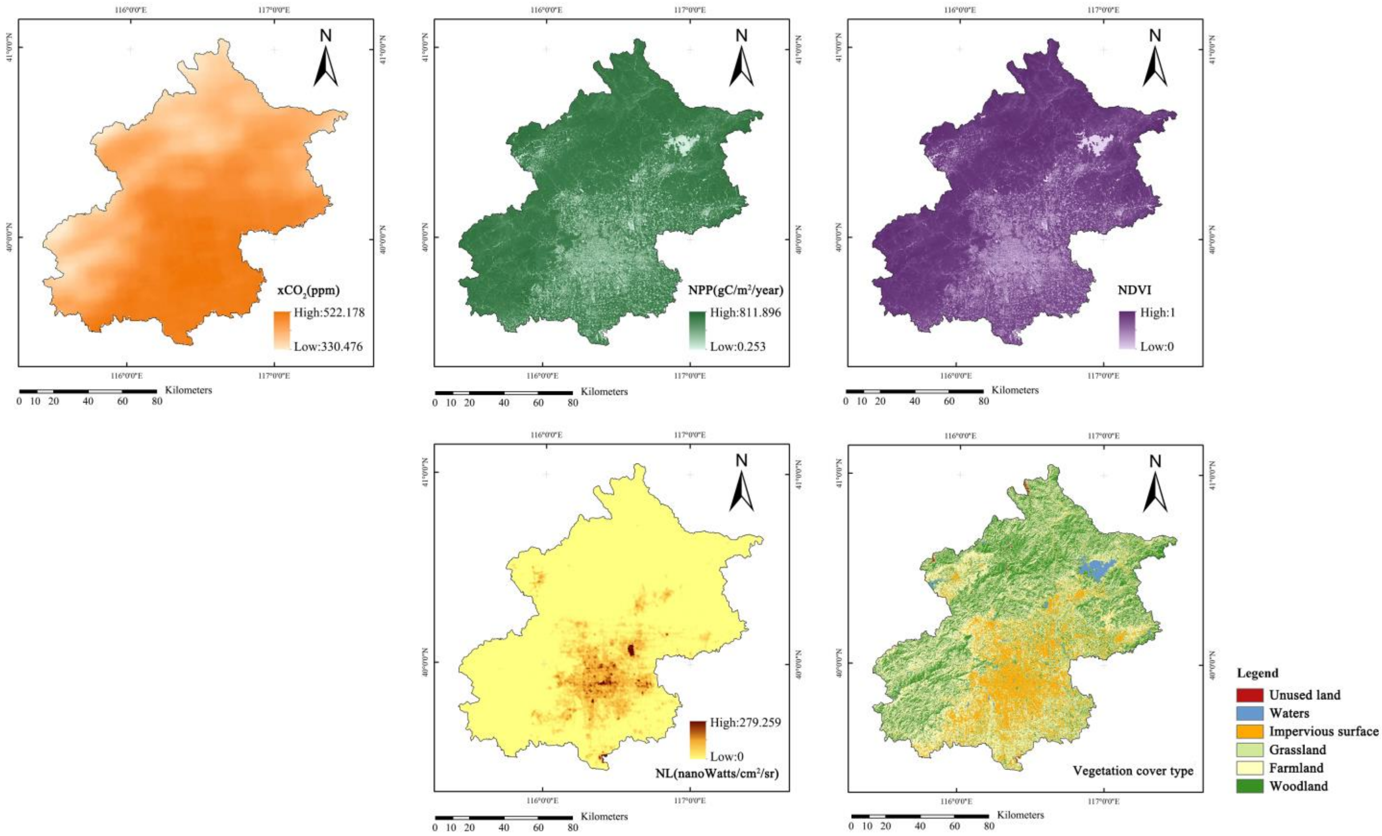

Figure 2. Spatial distribution of each impact factor.

Table 1. Various data categories, types, units of measurement, and data sources used in the study.

Data Type	Unit	Spatial Resolution	Data Source
Scope of administrative divisions in Beijing	/	/	www.tianditu.gov.cn accessed on 2 March 2023
30 m DEM elevation data in Beijing	/	30 m	www.gscloud.cn accessed on 2 March 2023
Beijing green space vector data	/	/	www.rivermap.cn accessed on 2 March 2023
Carbon dioxide concentration data (xCO_2)	ppm	2.25 km × 1.29 km	www.earthdata.nasa.gov accessed on 2 March 2023
Net primary productivity (NPP) data	$gC/m^2/year$	30 m	www.gisrs.cn accessed on 2 March 2023
Normalized difference vegetation index (NDVI)	/	30 m	https://doi.org/10.1016/j.rse.2019.111395 [41]
Satellite remote sensing images	/	30 m	www.gscloud.cn accessed on 2 March 2023
Night light (NL) data	$nanoWatts/cm^2/sr$	500 m	www.ngdc.noaa accessed on 2 March 2023

2.3. Research Methods

This study employs ArcGIS 10.5 as its primary research platform. The initial steps involve delineating the study area and defining the research objects. Subsequently, the carbon sink service radius is quantified using the buffer analysis method. The zoning statistical method is then applied to calculate potential impact factors that may affect the carbon sink service radius. Pearson correlation analysis is utilized to identify the driving factors contributing to the determination of the carbon sink service radius. The research results are analyzed to discern variations in the carbon sink service radius. The methodology and the process of handling and analyzing data in this study are illustrated in Figure 3. This approach ensures a comprehensive examination of the carbon sink service radius within the specified study area.

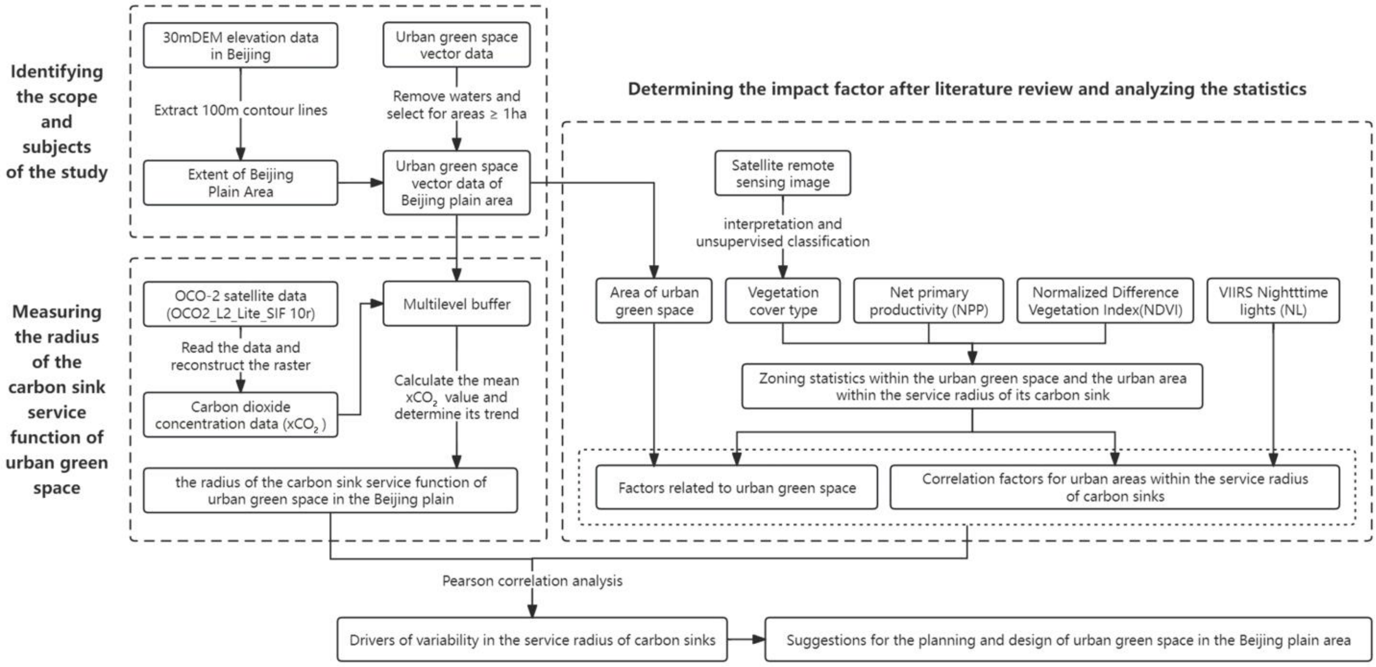

Figure 3. Research framework.

2.3.1. Calculation Method of the Carbon Sink Service Radius

Initially, considering the accuracy of CO_2 concentration data and the distribution of urban green spaces, a multi-level buffer analysis is conducted with urban green spaces as the center. The buffer zones start from the spatial boundaries of the green spaces, with a spacing of 1 km and a total length of 11 km, as illustrated in Figure 4. Average CO_2 concentrations within each buffer zone are obtained through zoning statistics and exported to Excel 2019. In the spreadsheet, the difference between the average CO_2 concentrations of adjacent buffer zones is calculated. If urban green spaces can reduce the CO_2 concentration in the surrounding urban areas, a trend of continuously rising CO_2 concentrations with increasing distance from the green spaces should be observed. Once the CO_2 concentration reaches the first peak and gradually decreases with distance, it is no longer considered within the range of the carbon sink service provided by urban green spaces. In Excel 2019, the SIGN function is employed to determine the trend of CO_2 concentration changes. The IF function is used to identify the first peak in CO_2 concentration changes, and the corresponding distance is assigned to the urban green space as its carbon sink service radius.

2.3.2. Calculation Method of Influencing Factors and Correlation Analysis

Due to variations in urban green spaces, including area, the composition of vegetation cover types, and surrounding urban areas, the carbon sink service radius exhibits differences. Initially, using ArcGIS 10.5, the area of each urban green space is obtained through geometric calculations. Zoning statistics are then applied to calculate NPP, NDVI, and the proportion of different vegetation cover types within urban green spaces. Considering that the carbon sink service radius is influenced not only by urban green spaces but also by surrounding urban areas, this study chooses to analyze influencing factors at both spatial levels: urban green spaces and the urban areas within their carbon sink service radius. This spatial zoning considers adjacent urban green spaces as part of the urban area, incorporating their impact on the carbon sink service radius into the urban area's indicators. This approach mitigates potential interference from mutual influences between adjacent urban green spaces. Given the diverse land-use types within urban areas, a multifactor analysis method is employed. Multiple factors related to carbon emissions and carbon sink, including average NPP, average NDVI, the proportion of different vegetation cover types, nighttime light index, and xCO_2, are selected.

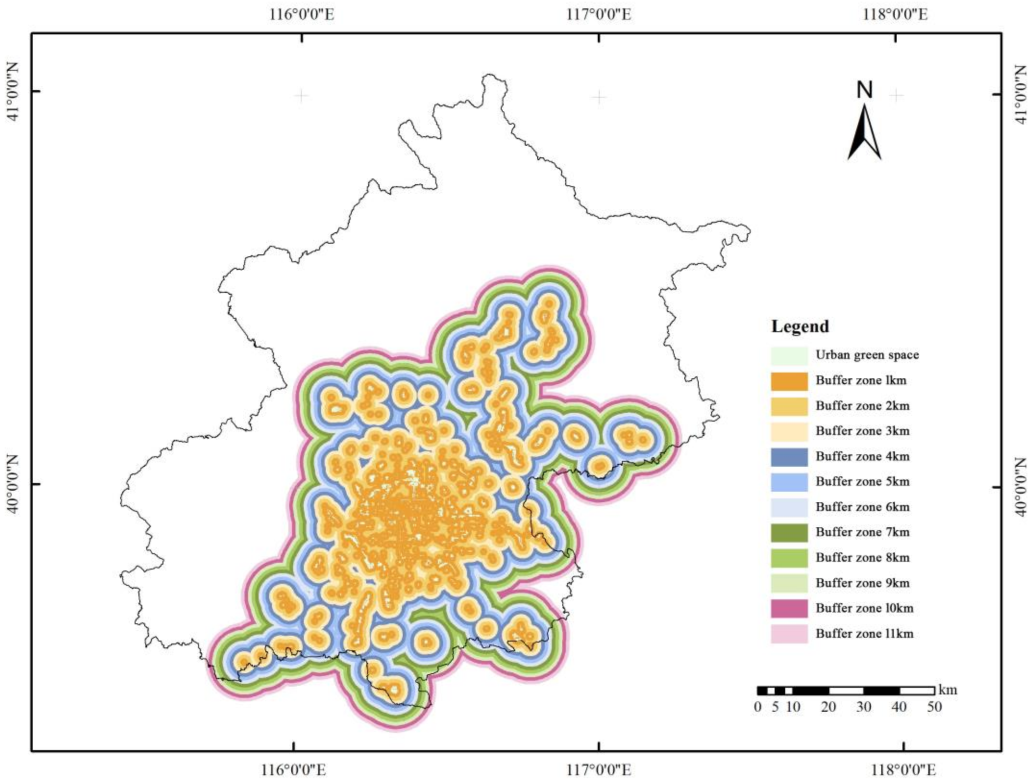

Figure 4. Spatial distribution of urban green space buffer zone.

To explore the causes of differences in the carbon sink service radius, this study uses influencing factors as independent variables and the carbon sink service radius as the dependent variable. Utilizing the SPSSPRO 1.1.13, Pearson correlation analysis and two-tailed t-tests are performed on the relevant factors to assess the significance of the relationship with the carbon sink service radius. The direction and degree of correlation coefficients are analyzed, leading to an attribution analysis of differences, thereby identifying factors influencing the size of the carbon sink service radius [42,43].

3. Results

3.1. Service Radius of Urban Green Space Carbon Sinks

In this study, 532 urban green spaces in the plain area were selected, and the carbon sink service radius could be calculated for 498 of them within a 10 km range. Figure 5 illustrates the spatial locations of urban green spaces and their carbon sink service radii. Figure 6 provides a breakdown of the quantity of urban green spaces with different carbon sink service radii. Notably, urban green spaces with a 1 km carbon sink service radius are the most numerous (110 in total), mainly concentrated in the central urban area along the Second Ring Road and a green belt, including parks like Ritan Park, Wanfeng Park, and Summer Palace. Urban green spaces with a 2 km carbon sink service radius are widely distributed in both the central urban area and suburbs, including parks like Yuantai Park, Guozhuang Park, and Grand Canal Forest Park. Those with a 3–5 km carbon sink service radius are concentrated in the southeast of Haidian District and the northwest of Chaoyang District, with the 4 km radius being particularly concentrated in the northwest of Chaoyang District, featuring parks like Yuanmingyuan, Olympic Forest Park (South), and Yuyuantan Park. Urban green spaces with a 6–7 km carbon sink service radius are mainly located in the eastern part of Chaoyang District, including parks such as Dongba Country Park, Pingfang Park, Dongfeng Park, and Xinglong Park. Those with an 8 km carbon sink service radius cover a significant portion of Haidian District, Dongcheng District, Xicheng District, Chaoyang District, and Shunyi District, including areas like Zhongshan Park, the North Garden of the National Botanical Garden, and Chaobai River Forest Park. Urban green spaces with a 9 km carbon sink service radius are the least numerous, mostly situated along green belts and in suburbs, like the South Garden of the National Botanical Garden. Finally, urban green spaces with a 10 km carbon sink service radius are concentrated in the central parts of Haidian District and Chaoyang District, featuring parks like Beiwu Park, Haidian Park, and Chaoyang Park.

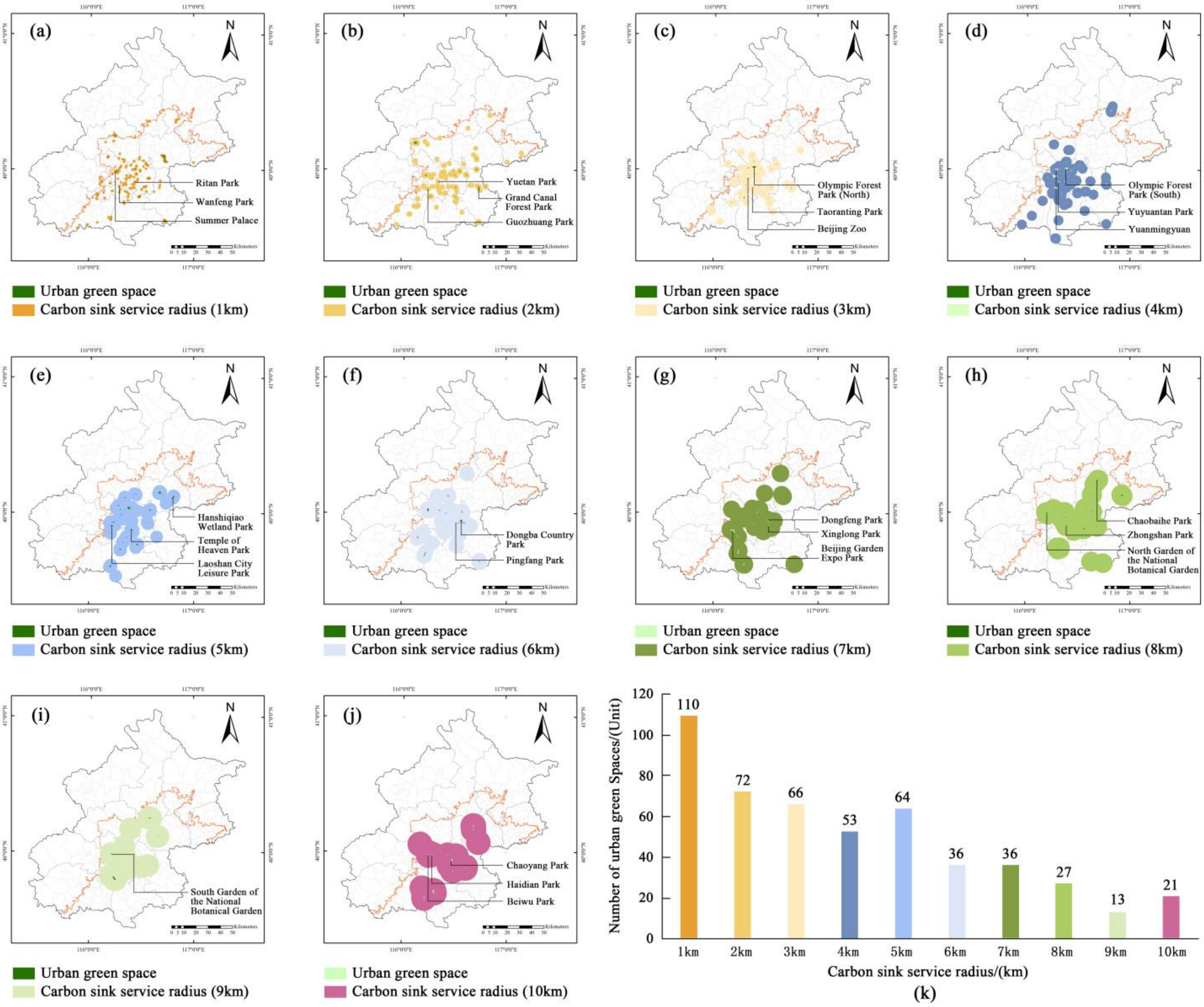

Figure 5. Measurement results of carbon sink service radius of urban green space. (**a**–**j**) Spatial distribution of urban green space and carbon sink service radius; (**k**) statistics of the carbon sink service radius of urban green spaces.

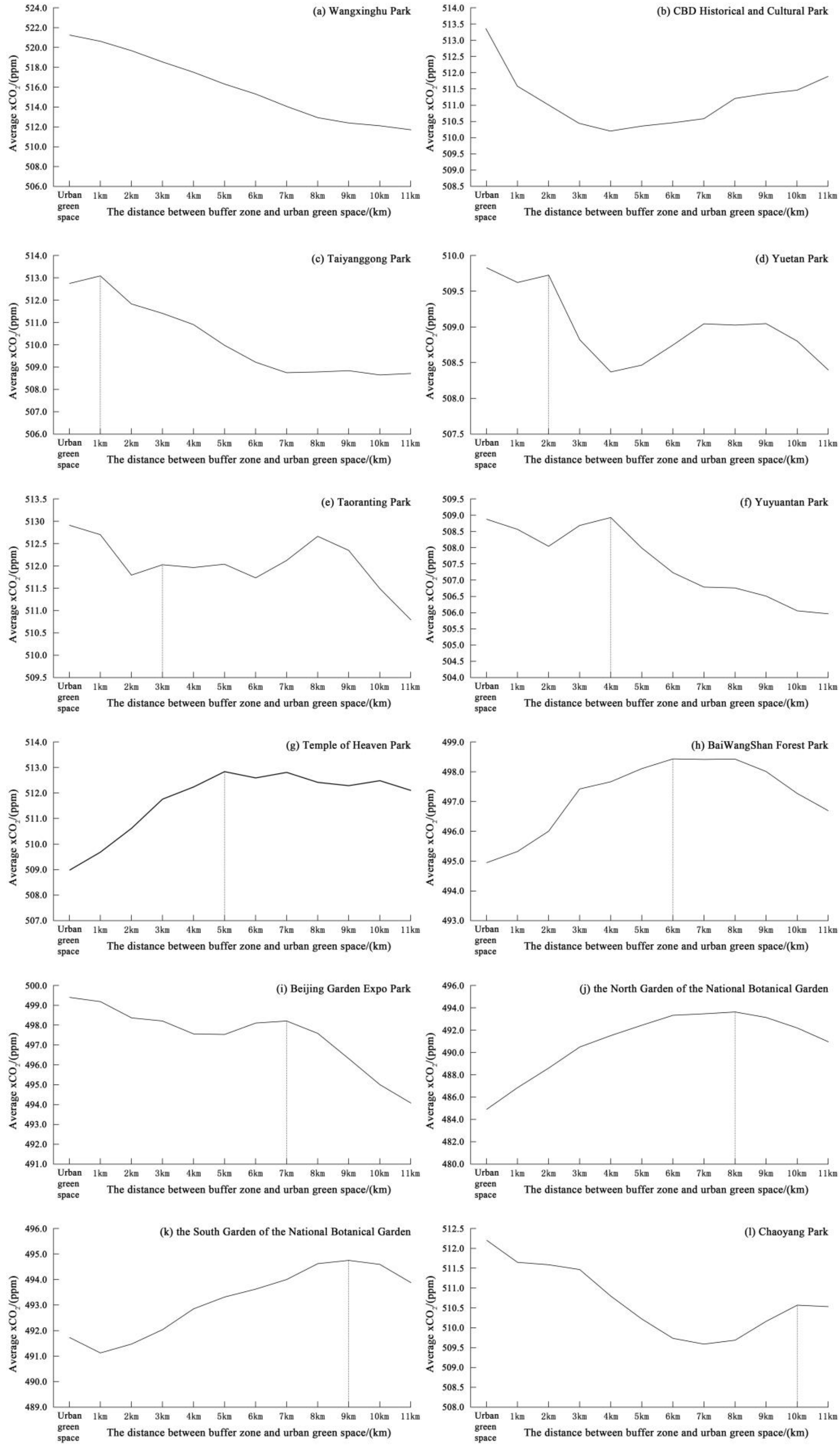

Figure 6. xCO_2 change trend around urban green space (typical cases).

Figure 6 reflects the changing trend of CO_2 concentration around some urban green spaces. In some cases, the xCO_2 concentration around urban green spaces continuously increases or decreases with distance, without reaching a CO_2 concentration peak within the 10 km range (Figure 6a,b). Other urban green spaces exhibit the first peak in CO_2 concentration within the range of 1 km to 10 km, allowing for the determination of their carbon sink service radius (Figure 6c–i). The variation in CO_2 concentration around urban green spaces may result from both the green spaces themselves and the surrounding urban areas. The carbon sink service radius may include other urban green spaces within it, and the urban areas within the radius may also contain spaces with carbon sink capabilities. These factors contribute to the extension of the carbon reduction effect of urban green spaces over a larger spatial range. When the CO_2 concentration shows a trend of initially increasing and then decreasing, it indicates that the urban green space has the lowest CO_2 concentration, and its effectiveness in reducing CO_2 concentration diminishes with increasing distance. After the carbon source and sink reach equilibrium, the trend of CO_2 concentration change reverses, forming the first peak (Figure 6c–h,j). When the CO_2 concentration first decreases and then increases, it may suggest that the urban area or adjacent urban green space is more effective in reducing CO_2 concentration (Figure 6d–f,i,k,l). When the synergistic effect of urban areas is too strong, the CO_2 concentration maintains its original trend over a larger spatial range. This trend surpasses the carbon reduction capability of urban green spaces, making it impossible to calculate the carbon sink service radius (Figure 6a,b).

3.2. Correlation Analysis between the Carbon Sink Service Radius and Influencing Factors

The correlation between each impact factor and the carbon sink service radius is shown in Table 2. The results of the study indicate that, among the indicators describing the characteristics of urban green spaces, the urban green space area exhibits a significant correlation with the carbon sink service radius at the 1% significance level, with a correlation index of 0.12. This suggests that increasing the area of urban green spaces effectively enhances the carbon sink service radius. The average NPP and average NDVI of urban green spaces do not show a significant correlation with the carbon sink service radius. This implies that changes in the net primary productivity and vegetation cover of urban green spaces are not the direct causes of changes in CO_2 concentration in the surrounding urban areas. Among the vegetation cover types of urban green spaces, only the proportion of grassland area exhibits a significant 10% correlation with the carbon sink service radius and shows a negative correlation, with a correlation index of -0.074. This indicates that an increase in the proportion of grassland area leads to a decrease in the carbon sink service radius. The proportions of forestland, cropland, and impervious surface area do not seem to be the causes of differences in the carbon sink service radius. In other words, regulating the proportions of these three vegetation cover types within urban green spaces does not have a direct impact on the size of the carbon sink service radius.

Regarding the indicators describing the characteristics of urban areas within the carbon sink service radius, the average NPP exhibits a significant positive correlation at the 1% significance level, with a correlation index of 0.095. The results suggest that an increase in the net primary productivity of urban areas can reduce CO_2 concentration in the atmosphere, leading to an expansion of the carbon sink service radius. The average NDVI of urban areas does not show a significant correlation with the carbon sink service radius. Thus, vegetation cover is not a direct cause of changes in CO_2 concentration and carbon sink service radius in urban areas. Among the related indicators of vegetation cover types, the proportions of forestland and grassland area exhibit significant positive correlations at the 1% significance level, with correlation indices of 0.121 and 0.125, respectively. This indicates that changes in the proportions of forestland and grassland area in urban areas have a significant impact on CO_2 concentration, causing variations in the carbon sink service radius. The proportion of impervious surface area shows a negative correlation, with a correlation index of -0.081, significant at the 10% level. Impervious surfaces typically correspond to urban construction land and are major sources of carbon in cities. Higher proportions of impervious surfaces are associated with a continuous maintenance of CO_2 concentration at relatively high levels in urban areas, leading to a decrease in the carbon sink service radius. The proportion of cropland area does not show a significant correlation with the carbon sink service radius, indicating that changes in its proportion do not directly affect CO_2 concentration in the atmosphere. The average NL, which can characterize human activity intensity, and average xCO_2 are not correlated with the size of the carbon sink service radius and do not cause changes in the carbon sink service radius.

Table 2. Correlation between the impact factors and the service radius of carbon sinks.

Scope of Statistics	Impact Factors	Correlation	Significance (Two-Tailed)
Urban green space	The area of urban green space	0.12	0.007 ***
	Average NPP	−0.019	0.678
	Average NDVI	0.024	0.597
	Proportion of forestland	0.051	0.253
	Proportion of grassland	−0.074	0.099 *
	Proportion of cultivated land	0.017	0.703
	Proportion of impervious surface	−0.021	0.645
Urban area within the carbon sink service radius	Average NPP	0.095	0.033 **
	Average NDVI	0.071	0.111
	Average NL	−0.031	0.484
	Average xCO_2	0.031	0.491
	Proportion of forestland	0.121	0.007 ***
	Proportion of grassland	0.125	0.005 ***
	Proportion of cultivated land	0.053	0.241
	Proportion of impervious surface	−0.081	0.073 *

Note: *** indicates significant correlation at the 1% level (two-tailed); ** indicates significant correlation at the 5% level (two-tailed); * indicates significant correlation at the 10% level (two-tailed).

4. Discussion

This study utilized xCO_2 as an indicator and applied the buffer zone method to analyze the variation trends in CO_2 concentration around urban green spaces. The study also calculated the carbon sink service radius of urban green spaces. Furthermore, from both the spatial perspectives of urban green spaces and the urban areas within their service radius, the study conducted a multifactor analysis of the correlation between factors influencing CO_2 concentration and the carbon sink service radius.

4.1. Urban Green Space Construction

The results of the study reveal a significant positive correlation between the area of urban green spaces and the carbon sink service radius. Previous research has indicated significant correlations between area and edge indicators, such as CA and AREA_MN, with NPP [44], aligning with our findings. Larger urban green spaces can provide more vegetation area to absorb and sequester CO_2, resulting in a larger carbon sink service radius. In contrast, smaller green spaces have limited capacity to absorb and fix CO_2, effectively reducing CO_2 concentration only in their immediate vicinity. For instance, Chaoyang Park, as the largest urban park within the Fourth Ring Road in Beijing, exhibits a carbon sink service radius of 10 km, while Ritan Park, with a smaller area, has a radius of 1 km. Additionally, studies suggest that while edge and shape metrics positively correlated with NPP, the fragmentation metrics were inversely related [45]. This means that the increased size and spatial continuity of urban green spaces enhance their carbon sink capacity. Human activities leading to reduced and fragmented green areas diminish carbon sink capabilities, impacting the ecological benefits of urban green spaces [46]. Hence, in urban planning and design, preserving existing green spaces and expanding their area with increased continuity is essential. The establishment of a comprehensive ecological network connecting different green spaces further contributes to enhancing overall carbon sink efficiency and promoting ecosystem health.

4.2. Carbon Sink Capacity Disparities

The study results indicate that urban green space NPP is not significantly correlated with the carbon sink service radius, whereas the carbon sink capacity of urban areas within the service radius shows a significant positive correlation. Spatial zoning statistics help distinguish the impact of different spatial units on the carbon sink service radius. For most urban green spaces, the area of urban areas within their influence range is much larger than the green space itself. The carbon sink service radius includes other urban green spaces and land types with carbon sink capabilities, contributing significantly more to carbon sink capacity than the green space alone. For example, Dongba Wild Park and the North Garden of the National Botanical Garden exhibit high similarity in area and vegetation cover type. However, due to the proximity of mountains near the North Garden of the National Botanical Garden, it has more carbon-intensive forestland, resulting in a larger carbon sink service radius than Dongba Wild Park.

Research also indicates that urban green space systems, through their rational arrangement and function, can reduce overall urban energy consumption, indirectly leading to emission reduction effects likely exceeding their carbon sink capabilities [47]. Therefore, the strategic planning of urban green space systems to maximize carbon sink capacity becomes a crucial issue in practice. Scholars have already predicted the green space structure of Beijing in 2035, reflecting future low-carbon development and ecological planning needs [48]. In the future, it is essential to consider both urban carbon reduction demands and the functional diversity of green spaces, setting reasonable green space construction goals within different spatial units [49]. By strengthening land governance, optimizing land use patterns, enhancing the quality and quantity of green space carbon sinks, and optimizing landscape patterns [50], significant contributions can be made to balancing the urban carbon system and mitigating climate change.

4.3. Influence of Vegetation Cover Types on the Carbon Sink Service Radius

Regarding the study of vegetation cover types, an increase in grassland area in urban green spaces may negatively impact the carbon sink service radius, while an increase in forest and grassland areas in urban areas contributes significantly to expanding the radius. Research indicates that lawns have poor carbon sequestration capabilities and may generate carbon emissions during maintenance processes [51]. This may explain the negative correlation between the proportion of grassland area in urban green spaces and the carbon sink service radius. In urban areas, forests play a crucial role as major regions with strong carbon sink capabilities. Studies demonstrate that tree-dominated biological communities exhibit high carbon sequestration efficiency and extensive carbon sequestration variability [52]. Moreover, some open green spaces with high tree coverage and planting density show efficiency comparable to densely vegetated closed green spaces [53]. This finding partially explains the positive impact of the proportion of grassland on the carbon sink service radius within urban areas. Despite the relatively weak carbon sink capacity of grassland in urban areas, it still plays a role in areas with concentrated carbon sources, contributing to improved carbon sink capacity.

However, impermeable surfaces such as buildings, roads, and artificial hardened surfaces are major carbon sources in urban areas. These surfaces usually lack vegetation cover, preventing photosynthesis for CO_2 absorption and fixation. The increase in impermeable surfaces not only limits the expansion of vegetation cover but may also lead to the urban heat island effect, influencing climate change [54]. When plant growth and photosynthetic efficiency are negatively affected, the plants' ability to absorb CO_2 is reduced [55], impacting the carbon sink service radius. Therefore, it is recommended to control grassland area reasonably in urban green space planning. In urban planning and construction, considerations should be given to vacating space, optimizing building density, improving land use efficiency, and reducing the increase of impermeable surfaces resulting from urban expansion [56]. Priority should be given to increasing the proportion of forest and grassland in urban areas, focusing on the planning and protection of forests to ensure sufficient trees and vegetation within urban areas, thereby enhancing carbon sink efficiency and expanding the carbon sink service radius.

5. Conclusions

Against the backdrop of carbon neutrality and the peak carbon target, China's ecological civilization construction has prioritized carbon reduction as a key strategic direction. This aims to facilitate a comprehensive green transformation of economic and social development, leading to a qualitative improvement in ecological environmental quality. Elevating the carbon sink capacity of urban green spaces has become a focal point in the new era of urban greening construction. This study employed the buffer zone analysis method to examine the variation trend of CO_2 concentration around urban green spaces with distance. It calculated the carbon sink service radius and quantified the actual impact of urban green spaces on reducing urban CO_2 concentration. Through spatial zoning statistics and multifactor analysis, this study investigated the disparities in carbon sink service radius. Overall, increasing the area of urban green spaces and the proportion of forests and grasslands within urban areas positively influences the carbon reduction efficacy of expanding urban green spaces. However, an increase in the proportion of grassland in urban green spaces and impermeable surfaces in urban areas negatively affects the carbon sink service radius. Given the characteristics of rapid construction, variable land use, and numerous construction indicators in the plains of Beijing, the research conclusions and recommendations are highly implementable and offer practical guidance. While acknowledging the potential limitations of employing buffer zone analysis and multifactor analysis in studying the carbon sink service radius and its disparities for urban green spaces, the research findings provide valuable insights from the perspective of carbon reduction effectiveness. These insights contribute to recommendations for urban green space construction in the plains of Beijing, holding significant implications for enhancing carbon sink capacity and achieving carbon neutrality and peak carbon targets. Additionally, future research could conduct quantitative analyses from the perspective of landscape pattern optimization, further enhancing our understanding of carbon sink services in urban green spaces. Exploring potential synergies with other ecosystem services, or integrating urban green space construction with various carbon sequestration or emission reduction measures could contribute to achieving sustainable green development in urban areas.

Author Contributions: Methodology, P.T.; resources, X.D.; data curation, J.L.; writing—original draft, S.G.; visualization, Z.Z.; supervision, P.Y. All authors have read and agreed to the published version of the manuscript.

Funding: This work was supported by the Project of Beijing Natural Science Foundation (grant number 8222022), the Hot Spot Tracking Project of Beijing Forestry University (grant number 2022BLRD08), the Science and Technology Innovation Program of Beijing Forestry University (grant number BLX202111), and the "Outstanding Young Talents" Cultivation Program of Beijing Forestry University (grant number 2019JQ03010).

Data Availability Statement: The data presented in this study are available on request from the corresponding author.

Conflicts of Interest: The authors declare no conflicts of interest.

References

1. Yoro, K.O.; Daramola, M.O. CO_2 emission sources, greenhouse gases, and the global warming effect. In *Advances in Carbon Capture*; Elsevier: Amsterdam, The Netherlands, 2020; pp. 3–28.
2. Rahman, M.N.; Wahid, M.A. Renewable-based zero-carbon fuels for the use of power generation: A case study in Malaysia supported by updated developments worldwide. *Energy Rep.* **2021**, *7*, 1986–2020. [CrossRef]

3. Ren, F.-R.; Tian, Z.; Liu, J.; Shen, Y.-T. Analysis of CO_2 emission reduction contribution and efficiency of China's solar photovoltaic industry: Based on Input-output perspective. *Energy* **2020**, *199*, 117493. [CrossRef]
4. Anika, O.C.; Nnabuife, S.G.; Bello, A.; Okoroafor, E.R.; Kuang, B.; Villa, R. Prospects of low and zero-carbon renewable fuels in 1.5-degree net zero emission actualisation by 2050: A critical review. *Carbon Capture Sci. Technol.* **2022**, *5*, 100072. [CrossRef]
5. Hong, W.Y. A techno-economic review on carbon capture, utilisation and storage systems for achieving a net-zero CO_2 emissions future. *Carbon Capture Sci. Technol.* **2022**, *3*, 100044. [CrossRef]
6. An, K.; Li, K.; Yang, C.-M.; Brechtl, J.; Nawaz, K. A comprehensive review on regeneration strategies for direct air capture. *J. CO_2 Util.* **2023**, *76*, 102587. [CrossRef]
7. National Academies of Sciences, Engineering, and Medicine. *Negative Emissions Technologies and Reliable Sequestration: A Research Agenda*; The National Academies Press: Washington, DC, USA, 2019.
8. Krzywanski, J.; Ashraf, W.M.; Czakiert, T.; Sosnowski, M.; Grabowska, K.; Zylka, A.; Kulakowska, A.; Skrobek, D.; Mistal, S.; Gao, Y. CO_2 capture by virgin ivy plants growing up on the external covers of houses as a rapid complementary route to achieve global GHG reduction targets. *Energies* **2022**, *15*, 1683. [CrossRef]
9. Gough, C.; Garcia-Freites, S.; Jones, C.; Mander, S.; Moore, B.; Pereira, C.; Röder, M.; Vaughan, N.; Welfle, A. Challenges to the use of BECCS as a keystone technology in pursuit of 1.5 °C. *Glob. Sustain.* **2018**, *1*, e5. [CrossRef]
10. López-Pacheco, I.Y.; Rodas-Zuluaga, L.I.; Fuentes-Tristan, S.; Castillo-Zacarías, C.; Sosa-Hernández, J.E.; Barceló, D.; Iqbal, H.M.; Parra-Saldívar, R. Phycocapture of CO_2 as an option to reduce greenhouse gases in cities: Carbon sinks in urban spaces. *J. CO_2 Util.* **2021**, *53*, 101704. [CrossRef]
11. Opinions of the Central Committee of the Communist Party of China and the State Council on Completely, Accurately, and Comprehensively Implementing the New Development Concept and Doing a Good Job of Carbon Peak and Carbon Neutrality. Available online: http://www.gov.cn/xinwen/2021-10/24/content_5644613.htm (accessed on 13 June 2023).
12. Notice of the Beijing Municipal People's Government on Issuing the Implementation Plan for Carbon Peak in Beijing. Available online: http://www.beijing.gov.cn/zhengce/zfwj/zfwj2016/szfwj/202210/t20221014_2836026.html (accessed on 14 June 2023).
13. Wang, Z.; Dong, X.; Shao, M.; Yao, P. Progress and Prospects of Research on Carbon Sink in Urban and Rural Green Spaces at Home and Abroad. *Landsc. Archit.* **2023**, *30*, 115–122.
14. Yin, K.; Tian, Y.; Yuan, C.; Zhang, F.; Yuan, Q.; Hua, L. NPP spatial and temporal pattern of vegetation in Beijing and its factor explanation based on CASA model. *Remote Sens. Land Resour.* **2014**, *27*, 133–139.
15. Tian, Y.; Huang, W.; Wu, X.; Jim, C.Y.; Wang, X.; Liu, Y. Dominant control of climate variations over land-use change on net primary productivity under different urbanization intensities in Beijing, China. *Acta Ecol. Sin.* **2019**, *39*, 416–424. [CrossRef]
16. Chen, Y.; Wang, J.; Xiong, N.; Sun, L.; Xu, J. Impacts of land use changes on net primary productivity in urban agglomerations under multi-scenarios simulation. *Remote Sens.* **2022**, *14*, 1755. [CrossRef]
17. Wang, B.; Wang, Y.; Zeng, C. Spatiotemporal Evolution of Carbon Sink Land in Changsha-Zhuzhou-Xiangtan Greenheart Area. *Econ. Geogr.* **2023**, *43*, 176–182+210.
18. Chen, Y.; Zhai, Y.; Gao, J. Spatial patterns in ecosystem services supply and demand in the Jing-Jin-Ji region, China. *J. Clean. Prod.* **2022**, *361*, 132177. [CrossRef]
19. Baró, F.; Haase, D.; Gómez-Baggethun, E.; Frantzeskaki, N. Mismatches between ecosystem services supply and demand in urban areas: A quantitative assessment in five European cities. *Ecol. Indic.* **2015**, *55*, 146–158. [CrossRef]
20. Hong, W.; Bao, G.; Du, Y.; Guo, Y.; Wang, C.; Wang, G.; Ren, Z. Spatiotemporal Changes in Supply–Demand Patterns of Carbon Sequestration Services in an Urban Agglomeration under China's Rapid Urbanization. *Remote Sens.* **2023**, *15*, 811. [CrossRef]
21. Wu, C.; Ju, Y.; Yang, S.; Zhang, Z.; Chen, Y. Reconstructing annual xCO_2 at a 1 km × 1 km spatial resolution across China from 2012 to 2019 based on a spatial CatBoost method. *Environ. Res.* **2023**, *236*, 116866. [CrossRef]
22. Lu, S.; Wang, J.; Wang, Y.; Yan, J. Analysis on the variations of atmospheric CO_2 concentrations along the urban–rural gradients of Chinese cities based on the OCO-2 xCO_2 data. *Int. J. Remote Sens.* **2018**, *39*, 4194–4213. [CrossRef]
23. Wang, Y.; Chen, W.; Kang, Y.; Li, W.; Guo, F. Spatial correlation of factors affecting CO_2 emission at provincial level in China: A geographically weighted regression approach. *J. Clean. Prod.* **2018**, *184*, 929–937. [CrossRef]
24. Keenan, T.; Williams, C. The terrestrial carbon sink. *Annu. Rev. Environ. Resour.* **2018**, *43*, 219–243. [CrossRef]
25. Cui, X.; Wei, X.; Liu, W.; Zhang, F.; Li, Z. Spatial and temporal analysis of carbon sources and sinks through land use/cover changes in the Beijing-Tianjin-Hebei urban agglomeration region. *Phys. Chem. Earth Parts A/B/C* **2019**, *110*, 61–70. [CrossRef]
26. Boulton, C.; Dedekorkut-Howes, A.; Byrne, J. Factors shaping urban greenspace provision: A systematic review of the literature. *Landsc. Urban Plan.* **2018**, *178*, 82–101. [CrossRef]
27. Ekkel, E.D.; de Vries, S. Nearby green space and human health: Evaluating accessibility metrics. *Landsc. Urban Plan.* **2017**, *157*, 214–220. [CrossRef]
28. Yu, Z.; Yang, G.; Zuo, S.; Jørgensen, G.; Koga, M.; Vejre, H. Critical review on the cooling effect of urban blue-green space: A threshold-size perspective. *Urban For. Urban Green.* **2020**, *49*, 126630. [CrossRef]
29. Su, J.G.; Dadvand, P.; Nieuwenhuijsen, M.J.; Bartoll, X.; Jerrett, M. Associations of green space metrics with health and behavior outcomes at different buffer sizes and remote sensing sensor resolutions. *Environ. Int.* **2019**, *126*, 162–170. [CrossRef] [PubMed]
30. Yang, H.; Zhong, X.; Deng, S.; Xu, H. Assessment of the impact of LUCC on NPP and its influencing factors in the Yangtze River basin, China. *Catena* **2021**, *206*, 105542. [CrossRef]

31. Liu, Y.; Liu, S.; Sun, Y.; Li, M.; An, Y.; Shi, F. Spatial differentiation of the NPP and NDVI and its influencing factors vary with grassland type on the Qinghai-Tibet Plateau. *Environ. Monit. Assess.* **2021**, *193*, 48. [CrossRef] [PubMed]
32. Wang, F.; Wang, Z.; Zhang, Y. Spatio-temporal variations in vegetation Net Primary Productivity and their driving factors in Anhui Province from 2000 to 2015. *Acta Ecol. Sin.* **2018**, *38*, 2754–2767.
33. Liu, Q.; Song, J.; Dai, T.; Shi, A.; Xu, J.; Wang, E. Spatio-temporal dynamic evolution of carbon emission intensity and the effectiveness of carbon emission reduction at county level based on nighttime light data. *J. Clean. Prod.* **2022**, *362*, 132301. [CrossRef]
34. Zhou, Y.; Chen, M.; Tang, Z.; Mei, Z. Urbanization, land use change, and carbon emissions: Quantitative assessments for city-level carbon emissions in Beijing-Tianjin-Hebei region. *Sustain. Cities Soc.* **2021**, *66*, 102701. [CrossRef]
35. Pan, R.; Zheng, X. *Study on the Impact of Million mu Afforestation Project on Carbon Storage in Terrestrial Ecosystem—A Case Study of Beijing Plain Area*; China Architecture & Building Press: Changsha, China, 2022.
36. Yang, W.; Li, J.; Wen, C.; Huang, Y.; Gu, Y.; Zhu, J.; Tang, Y. Building ecological networks in Beijing Plain based on local species distribution. *Acta Ecol. Sin.* **2022**, *42*, 8213–8222.
37. Li, Z.; Ziyi, L.; Xinyao, M.; Shan, L. Effects of Plant Community Characteristics on Carbon Sequestration Efficiency in Urban Parks. *Landsc. Archit. Acad. J.* **2023**, *40*, 125–134.
38. Wei, X.; Yang, J.; Luo, P.; Lin, L.; Lin, K.; Guan, J. Assessment of the variation and influencing factors of vegetation NPP and carbon sink capacity under different natural conditions. *Ecol. Indic.* **2022**, *138*, 108834. [CrossRef]
39. Baniya, B.; Tang, Q.; Huang, Z.; Sun, S.; Techato, K.-A. Spatial and temporal variation of NDVI in response to climate change and the implication for carbon dynamics in Nepal. *Forests* **2018**, *9*, 329. [CrossRef]
40. Zhao, J.; Ji, G.; Yue, Y.; Lai, Z.; Chen, Y.; Yang, D.; Yang, X.; Wang, Z. Spatio-temporal dynamics of urban residential CO_2 emissions and their driving forces in China using the integrated two nighttime light datasets. *Appl. Energy* **2019**, *235*, 612–624. [CrossRef]
41. Yang, J.; Dong, J.; Xiao, X.; Dai, J.; Wu, C.; Xia, J.; Zhao, G.; Zhao, M.; Li, Y.; Zhang, Y.; et al. Divergent shifts in peak photosynthesis timing of temperate and alpine grasslands in China. *Remote Sens. Environ.* **2019**, *233*, 111395. [CrossRef]
42. Gogoi, A.; Ahirwal, J.; Sahoo, U.K. Evaluation of ecosystem carbon storage in major forest types of Eastern Himalaya: Implications for carbon sink management. *J. Environ. Manag.* **2022**, *302*, 113972. [CrossRef]
43. Qiu, C.; Wang, C.; Zhang, R. Characteristics of ecological space carbon sequestration service function and its relationship with landscape pattern in Beijing-Tianjing-Hebei urban agglomeration. *Acta Ecol. Sin.* **2022**, *42*, 9590–9603.
44. Tao, P.; Lin, Y.; Wang, X.; Li, J.; Ma, C.; Wang, Z.; Dong, X.; Yao, P.; Shao, M. Optimization of Green Spaces in Plain Urban Areas to Enhance Carbon Sequestration. *Land* **2023**, *12*, 1218. [CrossRef]
45. Kabisch, N.; Qureshi, S.; Haase, D. Human–environment interactions in urban green spaces—A systematic review of contemporary issues and prospects for future research. *Environ. Impact Assess. Rev.* **2015**, *50*, 25–34. [CrossRef]
46. Yang, H.; Chen, W. Spatio-temporal pattern of urban vegetation carbon sink and driving mechanisms of human activities in Huaibei, China. *Environ. Sci. Pollut. Res.* **2022**, *29*, 31957–31971. [CrossRef] [PubMed]
47. Shi, N.; Yu, Y.; Liang, S.; Ren, Y.; Liu, M. Effects of urban green spaces landscape pattern on carbon sink among urban ecological function areas at the appropriate scale: A case study in Xi'an. *Ecol. Indic.* **2024**, *158*, 111427. [CrossRef]
48. Liu, Y.; Xia, C.; Ou, X.; Lv, Y.; Ai, X.; Pan, R.; Zhang, Y.; Shi, M.; Zheng, X. Quantitative structure and spatial pattern optimization of urban green space from the perspective of carbon balance: A case study in Beijing, China. *Ecol. Indic.* **2023**, *148*, 110034. [CrossRef]
49. Xu, L.; Fang, K.; Huang, Y.; Xu, S. Demand priority of green space from the perspective of carbon emissions and storage. *Sustainability* **2023**, *15*, 11199. [CrossRef]
50. Li, H.; Xie, X.; Li, C. Carbon Sink Effects and Optimization Suggestions for Landscape Patterns in the Chengdu-chongqing Twin Cities Region: BP Neural Network-based Analysis and Prediction. *Urban Dev. Stud.* **2023**, *30*, 92–102.
51. Zhang, Y.; Meng, W.; Yun, H.; Xu, W.; Hu, B.; He, M.; Mo, X.; Zhang, L. Is urban green space a carbon sink or source?—A case study of China based on LCA method. *Environ. Impact Assess. Rev.* **2022**, *94*, 106766. [CrossRef]
52. De la Sota, C.; Ruffato-Ferreira, V.; Ruiz-García, L.; Alvarez, S. Urban green infrastructure as a strategy of climate change mitigation. A case study in northern Spain. *Urban For. Urban Green.* **2019**, *40*, 145–151. [CrossRef]
53. Wang, Y.; Chang, Q.; Li, X. Promoting sustainable carbon sequestration of plants in urban greenspace by planting design: A case study in parks of Beijing. *Urban For. Urban Green.* **2021**, *64*, 127291. [CrossRef]
54. Wardeh, Y.; Kinab, E.; Escadeillas, G.; Rahme, P.; Ginestet, S. Review of the optimization techniques for cool pavements solutions to mitigate Urban Heat Islands. *Build. Environ.* **2022**, *223*, 109482. [CrossRef]
55. Dusenge, M.E.; Duarte, A.G.; Way, D.A. Plant carbon metabolism and climate change: Elevated CO_2 and temperature impacts on photosynthesis, photorespiration and respiration. *New Phytol.* **2019**, *221*, 32–49. [CrossRef]
56. Rahaman, Z.A.; Kafy, A.-A.; Saha, M.; Rahim, A.A.; Almulhim, A.I.; Rahaman, S.N.; Fattah, M.A.; Rahman, M.T.; Kalaivani, S.; Al Rakib, A. Assessing the impacts of vegetation cover loss on surface temperature, urban heat island and carbon emission in Penang city, Malaysia. *Build. Environ.* **2022**, *222*, 109335. [CrossRef]